Analytica Chimica Acta, 282 (1993) 239–246
Elsevier Science Publishers B.V., Amsterdam

Investigation of silver iodide-based ion-selective membranes by scanning electrochemical microscopy

Klára Tóth and Géza Nagy

Institute for General and Analytical Chemistry, Technical Analytical Research Group of the Hungarian Academy of Sciences, Technical University of Budapest, H-1111 Budapest (Hungary)

Benjamin R. Horrocks and Allen J. Bard

Department of Chemistry and Biochemistry, The University of Texas at Austin, Austin, TX 78712 (USA)

(Received 9th August 1993)

Abstract

The proton concentration–distance profile developed at the interface of silver iodide-based solid-state electrodes in corroding cyanide solutions of low buffer capacity has been studied by scanning electrochemical microscopy using a potentiometric tip. The experimental results verified the theory developed earlier for the interpretation of the operation mechanism of "corrosion" type electrodes.

Keywords: Ion-selective membranes; Scanning electron microscopy; Silver iodide

Solid-state ion-selective electrodes based on silver iodide or a mixture of silver iodide and silver sulphide have been widely used to monitor the cyanide ion concentration in different matrices (e.g. [1–4]). The operational model of silver halide electrodes responding to complex forming ligands such as cyanide has been elaborated on the basis of a dissolution or "corrosion" reaction between the silver halide (AgX) and the cyanide and has been discussed in a number of articles [1,2,5–9]. Accordingly the silver halide-based sensors have a cyanide response, through sensing the halide ions generated in a surface reaction such as:

$$AgX + 2CN^- \rightarrow Ag(CN)_2^- + X^- \quad (1)$$

Safety reasons dictate that cyanide measurements should be made in strongly basic solutions (pH > 11), where volatile HCN is not present. However, it is obvious that the pH can affect the potential response of the electrode to cyanide. The electrode potential vs. pH dependence has been studied experimentally and the early observations could be interpreted on the basis of protolytic equilibria and the corrosion reaction [1,2]. For use in monitoring enzyme catalysed processes generating cyanide the pH cannot be selected at random. A pH value providing good stability and high catalytic activity for the enzymatic reaction is a prerequisite. Mascini [10] investigated cyanide-cleaving enzyme reactions with a cyanide ion-selective electrode. The experimental electrode potential vs. pH curves thus recorded in highly buffered cyanide solutions were not in complete agreement with earlier observations [10]. To obtain a better understanding about the mechanism, detailed experimental studies on the pH dependence of the cyanide electrode response were carried out. The results of these experiments

Correspondence to: K. Tóth and A.J. Bard at the above addresses.

revealed that in the pH range 5–9 the potential of the cyanide electrode depends not only on the cyanide ion activity and pH but also strongly on the buffer capacity of the solution [11].

In the early work, surface iodide concentration values were calculated by considering the cyanide concentrations and the dissociation constants of the relevant complex and the weak acid taking part in the corrosion process. By substituting these concentration values into the Nernst equation, the theoretical electrode potential vs. pH curves were calculated [7,10–12]. However, the experimental curves in the case of low buffer capacities showed a poor fit to this curve. This finding could be explained by taking into account the reaction:

$$AgX + 2HCN \rightarrow Ag(CN)_2^- + 2H^+ + X^- \qquad (2)$$

and the generated local concentration profiles [11].

In the lower pH range reaction 2 competes with reaction 1 at the membrane surface and as the "corrosion" dissolution reaction proceeds, the iodide (X^-), the dicyanoargentate and also the hydrogen ion concentrations increase while the cyanide concentration decreases in the vicinity of the electrode membrane–solution interface. A concentration gradient will build up and transport processes driven by it will take place. In quiescent solution the diffusion and natural convection produce the concentration profile, while in stirred solution it is convective diffusion. Under steady state conditions the surface iodide concentration, which is dependent on the bulk cyanide and hydrogen ion concentrations, determines the response function.

When reaction 2 occurs, as discussed above, the solution layer in direct contact with the membrane would be more acidic than the bulk of the solution. The pH difference between the vicinity of the membrane surface and the bulk is naturally buffer-capacity dependent, and becomes larger as the buffer capacity of the solution decreases. Thus, the buffer capacity can influence the surface iodide activity and consequently the potential of the silver iodide electrode. The difference between the measured and the calculated pH–cyanide activity dependent response curves originates from the pH gradient.

Attempts made to verify the above explanation, namely the existence of a local pH gradient at the solution–electrode membrane interface by ordinary chromogenic indicators were successful [13]. The change in pH with distance from the interface under different circumstances, however, could not be measured experimentally.

The processes taking place at the surface of corrosion-type cyanide electrodes have been studied with different surface analytical methods such as photoelectron spectroscopy, scanning electron microscopy and x-ray fluorescence spectrometry [14]. With these methods the surface of the untreated and pretreated and consequently dried membranes could be investigated in a vacuum. Changes in the composition of the solid membrane surfaces caused by treatment such as conditioning in solutions of different compositions for different time periods could be detected. However, no information could be gathered about the concentration profiles at the solution–membrane interface.

With the development of scanning electrochemical microscopy (SECM) employing an ultramicro voltammetric electrode, a new tool has become available to obtain chemical information about conductive and non-conductive substrates, to study electrode surfaces with high spatial resolution and kinetics of surface reactions [15]. Recent progress in the fabrication of a pH-selective potentiometric tip for SECM has provided a new way to investigate local pH effects of different reactions which are not accessible with microvoltammetric tips and amperometric techniques. The smallness of the potentiometric tip allows surfaces to be imaged with high spatial resolution and concentration profiles to be monitored precisely.

In amperometric SECM a precise tip-substrate (target) distance calibration method has been elaborated [16]. It operates by comparing the amperometric signal with a theoretically derived and experimentally well-proved current–distance calibration curve. In the case of SECM with a potentiometric tip, the signal from the tip can not be used for distance calibration. Therefore a separate independent method is needed for the determination of the absolute tip to target surface

distance for the effective use of potentiometric SECM. It has been proved that the antimony microdisc electrode can be used in both amperometric and potentiometric microscopy. In this way the distance calibration can be made in the amperometric mode while the pH imaging can be performed in the potentiometric mode [17].

Antimony pH electrodes are well known and are widely used in different areas when glass electrodes are inappropriate, e.g., in fluoride media or in the food industry. The properties of antimony electrodes have been reviewed recently [18]. The micro versions of antimony pH electrodes, employed mostly in different areas of experimental life sciences, are fabricated as very thin-walled capillaries to facilitate penetration and minimise invasion [19,20]. For microscopy a more durable and polishable design is needed which has a well-defined tip geometry to allow mass transport-based distance calibration. An antimony microdisc electrode for SECM has recently been described [17].

The purpose of the study reported here was to monitor proton concentration profiles in solutions of different buffer capacities generated above an AgI surface by the corrosion reaction and to provide in situ evidence for the assumption given in an earlier publication [11,14] in order to interpret the cyanide electrode response function in weakly buffered media.

EXPERIMENTAL

Instrumentation

A recent, slightly modified version of the basic scanning electrochemical microscope capable of performing both potentiometric and amperometric imaging [17] was used in these investigations.

The instrument used three piezoelectric inchworm motors for high precision three dimensional positioning (Burleigh Instruments, Fishers, NY). Their movement was controlled by a PC via an analog-to-digital converter (ADC). The cell holder contained two inchworm positioners which moved the cell in the horizontal x or y direction, while the measuring tip was mounted on the vertical (z) motor. The amperometric microscopy set used an EI-400 bipotentiostat (Ensman Instrument, Bloomington, IN) as the measuring apparatus. For potentiometric microscopy a home-built high-impedance voltmeter was used to measure the potential difference between the tip and a conventional 0.1 M silver/silver chloride reference electrode located in the bulk of the solution. In both operation modes the output of the measuring instrument was fed into one of the channels of the ADC board to allow data acquisition by computer for image formation.

The cell was a shallow conical PTFE cup with a volume of ca. 4 ml. Its wide mouth allowed easy observation during manual approximate positioning of the tip. The narrower cell bottom, which screwed into the cell body, was used as a target holder. The cylindrical sample targets were mounted in the cell by tight fitting into a hole bored through the cell bottom. The auxiliary electrode used for amperometric measurements was a platinum wire of 0.5 mm diameter entering the cell through the PTFE cell wall.

For electrochemical characterisation of antimony electrodes a BAS 100A potentiostat was used. The pH measurements were performed with an Orion pH meter (Model 701A).

Targets

To achieve a true steady state concentration profile around the silver iodide surface in cyanide solutions, glass shield inlaid microdisc silver iodide targets were made. To prepare such targets, glass capillaries were sealed at one end in a flame with slow rotation to achieve a gradual tapering of the capillary bore toward the sealed end. Finely ground, dry silver iodide powder (for preparation see below) was introduced inside the capillary and was compacted by drop hammering inside a guide tube, and subjected to a vacuum. The silver iodide was carefully melted under vacuum by holding the closed end of the tube in a microflame. After letting it cool down slowly, the sealed end was polished to expose a small circular silver iodide disc (diameter 25–120 μm) in the middle of a flat glass surface of ca. 2 mm diameter. After polishing, the microelectrode targets were inserted into the base of the cell as outlined above.

Electrode fabrication

Pressed pellets of silver iodide used to prepare membrane discs (5 mm diam., 6 mm thick) were made of silver iodide precipitate pressed at 10^9 Pa. These pellets were incorporated into Philips solid state electrode bodies. The internal filling solution was 0.1 M KNO_3, 1 mM $AgNO_3$ and the internal reference electrode was a chloride coated silver wire.

The silver iodide used for the preparation of the discs was precipitated by titration of stirred 0.1 M silver nitrate with 0.1 M sodium iodide dropwise under careful potentiometric control. An iodide-selective indicator electrode (Radelkis Type OP-I-7111D) and a silver/silver chloride double junction reference electrode (Radelkis Type OP-8202) was used for end-point detection. The precipitate obtained was aged by standing for 24 h, washed three times with distilled water and dried in an oven at 105°C for 3 h.

The illustrated, step by step procedure for antimony SECM tip fabrication is given elsewhere [17]. Here a short description only is given. Antimony shot (99.999%, Aldrich, Milwaukee, WI) was melted and sucked into a thick-walled Pyrex capillary (outer diameter, 7 mm, inner diameter, 1 mm). With standard glassblowing techniques, antimony-filled capillaries of outside diameter in the 1–2 mm range were pulled manually. It is advisable to heat up the end of the capillary and use tweezers for rapid pulling. In this way the build up of excess pressure in the column of antimony and deformation of the capillary can be avoided. A section of the antimony-filled capillary, about 50 mm long, was carefully selected under optical microscope view. (The antimony fiber inside must be continuous with a diameter of 20–100 μm.) These capillaries were pulled again using the heating coil of a microelectrode puller (Stoelting). A small weight (1–2 g) was attached to one end of the antimony capillary. The voltage applied to the coil was manually controlled observing the extension of the heated section of the capillary. A short tapered section of the capillary obtained was mounted in another glass capillary serving as a holding body. A well-defined disc of antimony was exposed by gently scoring near the end of the capillary and carefully breaking the capillary against a fingertip. Electrical contact was made by mercury introduced through the back of the supporting capillary. The relatively thick glass wall (total diameter to disc diameter ratio = 5 to 10) of these small capillaries allows careful polishing (with MOYCO, Ultralap aluminacoated strips). Electrodes with an antimony disc down to 3 μm diameter were made in this way. For preparation of electrodes with a smaller disc diameter the double pulled glass-coated antimony fibers were sealed under vacuum in low melting point glass, as is commonly done in the preparation of microdisc electrodes from platinum wire [21]. The antimony fiber-containing glass rods prepared in this way can be pulled down for size reduction, bevelled and polished.

RESULTS AND DISCUSSION

Electrode characterisation

The pH function of the shielded microdisc antimony electrodes was carefully studied with different buffer systems. A typical calibration graph obtained for a series of phosphate buffers is linear and has the equation $E = (-108.6 - 45.5$ pH) mV. The diameter of the antimony microdisc was 6 μm and a saturated calomel electrode was used as a reference electrode. The electrode showed no change of potential at pH 7 when changing the phosphate concentration in the range of 1–100 mM. The slopes of the calibration graphs obtained with different electrodes were typically between 40 and 50 mV per pH. This is the usual slope value for a polycrystalline antimony electrode. Different treatments suggested in the literature, such as soaking in oxidising agents (permanganate or dichromate) or anodization under different conditions, were tried in order to improve the slope of the pH function. However, no significant success was achieved. Therefore the antimony tips were used in microscopy without special pretreatment.

It was observed that after voltammetric experiments, especially if the antimony tip was negatively polarised for long times, the pH measuring function was lost (the electrode potential drifted,

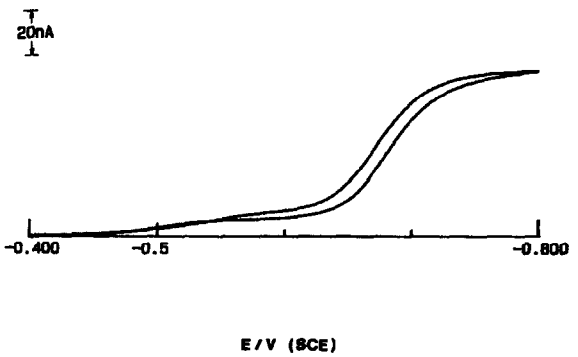

Fig. 1. Cyclic voltammogram of methyl viologen (9.1 mM in argon purged 0.1 M KCl; polarising rate, 10 mV s^{-1}).

the slope of the pH calibration graph decreased and the reproduction of the potential value became poor). The reason for this is the reduction of the oxide film at the electrode surface. The pH function of the antimony electrode was restored after a few hours in air, or soaking in oxidising solutions. The easiest way to restore the pH function, however, was to polarize the tip for a few seconds to 0 V. After this, the original pH function of the electrode was regained. Reproducible behaviour was observed for any individual microelectrode prepared as described; the calibration points were found to be within a few mV when measured on different days. While the oxygen concentration was changed in the cell by bubbling nitrogen gas, no significant change in the electrode potential was observed.

For tip–substrate distance calibration, amperometric measurements can well be used in scanning electrochemical microscopy [16,17]. To investigate the applicability of the antimony tip in this respect voltammetric measurements were carried out. Fig. 1 shows a cyclic voltammogram of 9.1 mM methylviologen in argon purged 0.1 M KCl at a 25-μm diameter antimony tip. The half-wave potential is in agreement with the formal potential (−0.68 V vs. SCE) and the voltammogram has the characteristic sigmoidal shape expected for a microelectrode. Making several cycles or keeping the electrode potential on the plateau for a longer period did not produce noticeable changes of the electrochemical activity of the electrode surface. This guaranties that the

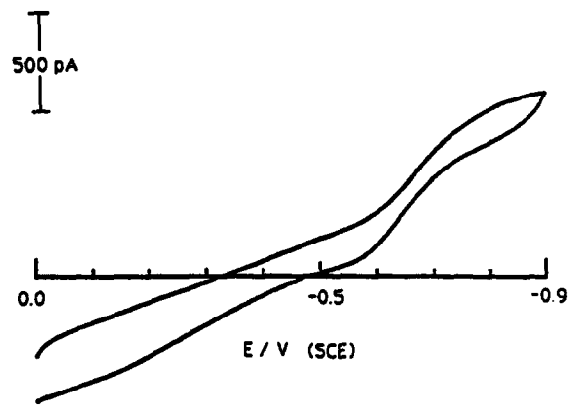

Fig. 2. Cyclic voltammograms of an antimony microelectrode of 3 μm diameter in air-saturated 1 mM (pH 7.0) phosphate buffer containing 0.1 M KCl. Sweep rate: 100 mV s^{-1} [17].

distance calibration can be made with the antimony measuring tip in the amperometric mode.

In order to avoid the need of adding an external redox couple to the sample solution, the use of oxygen reduction for distance calibration was attempted. Fig. 2 [17] shows a cyclic voltammogram prepared in air-saturated phosphate buffer, pH 7.0. The oxygen reduction wave is clearly defined. It was also verified with nitrogen purging. Setting the potential of the microelectrode between −0.7 and −0.9 V a steady state current was obtained which reflected well the oxygen concentration in the solution.

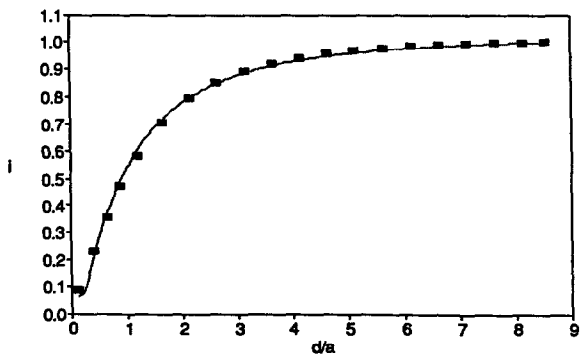

Fig. 3. Current-distance (i_T–d) curve (i_T normalized to $i_{T\infty}$ and d to the radius of the tip, a) for a 4 μm diameter antimony microdisc operating in amperometric mode. The solution was 0.1 M (pH 7.0) phosphate buffer containing 0.1 M KCl, while the sample surface was a PTFE disc. Solid line = experimental data; and ■ = theoretical values [17].

For tip–substrate distance calibration the electrode potential was set to −0.8 V and air-saturated buffer solution was introduced into the PTFE cell. The oxygen reduction current was monitored while the electrode approached the PTFE substrate surface. The experimental current–distance curve is shown in Fig. 3 (solid line) [17]. It can be seen that while the tip is far from the target surface, the current is constant. When it approaches the surface, owing to the irreversible character of oxygen reduction and the blocking or shielding effect ("negative feedback" [15,16]) of the surface on the oxygen diffusion to the electrode, the current decreases. The good fit of the theoretical points to the experimental curve proves that the oxygen reduction curve on the antimony tip allows the measurement of absolute tip–surface distance [17].

The amperometric distance calibration is very advantageous especially if the oxygen reduction current is used. In this case no redox agent addition is necessary. An external additive can easily interfere with the system investigated or with the pH measuring function of the antimony electrode. For the amperometric distance measurement no knowledge of the diffusion coefficient, concentration or stoichiometry of the electrochemical reduction of the material, here the oxygen, is required.

Potentiometric studies with a silver iodide membrane electrode

To investigate the pH dependence of the cyanide electrode function in buffered or unbuffered cyanide solutions, the pH of the test solution was adjusted to high values by adding solid potassium hydroxide. The potential of the silver iodide based cyanide electrode and of a pH measuring glass electrode immersed in the solution were recorded while, by adding portions of nitric acid the pH was gradually decreased. To avoid hydrogen cyanide loss the measurements were performed in a closed cell. The potential of the cyanide electrode was plotted as a function of bulk pH measured. The experimentally observed plots ranged between two limiting cases. In highly buffered media when the cyanide concentration was relatively low the electrode potential–pH

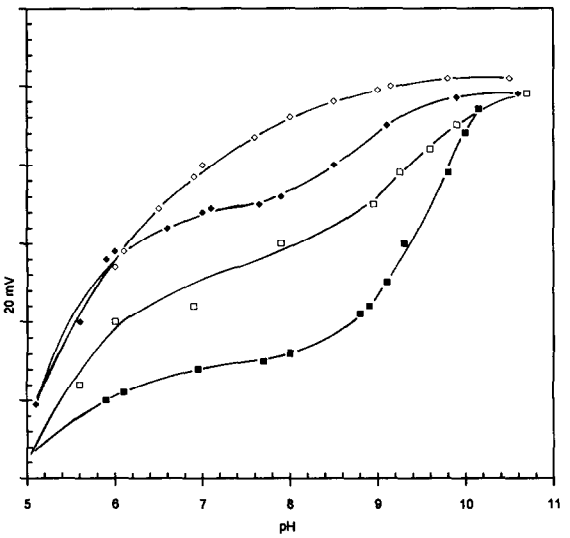

Fig. 4. Electrode potential vs. pH curves for a silver iodide based cyanide electrode in 10^{-3} M KCN solutions of different buffer capacities. ◇, 10^{-1} M Britton Robinson buffer; ◆, 10^{-3} M Britton Robinson buffer; □, 10^{-5} M Britton Robinson buffer; ■, no buffer is added. All solutions contained 0.1 M KCl too. Reference electrode was a double junction Ag/AgCl electrode, Radelkis Type OP-8202.

curve showed theoretical behaviour: that means it could be described by the earlier mentioned equation [10,11], i.e.,

$$E = E_I^0 - S \log \frac{K_{HCN}\sqrt{K}\, a_{CN,t}}{K_{HCN}(2\sqrt{K}+1) + a_H} \qquad (3)$$

where S is the slope of the cyanide electrode calibration graph, E is the potential of the cyanide electrode, E_I^0 is the standard potential, K_{HCN} is dissociation constant of HCN (4.8×10^{-10} M), K is the equilibrium constant for

$$AgI + 2CN^- \rightleftarrows Ag(CN)_2^- + I^- \qquad (4)$$

the surface reaction ($K = 6.28 \times 10^4$ M), a is the ion activity, t stands for total ($a_{CN,t} = a_{CN^-} + a_{HCN}$).

The other limiting case is obtained in the absence of external buffer. Experimentally obtained electrode potential–pH curves are shown in Fig. 4. As can be seen in the case of the low buffer capacity media in the pH range 5–10 the measured electrode potential is more positive than is expected theoretically or is observed at

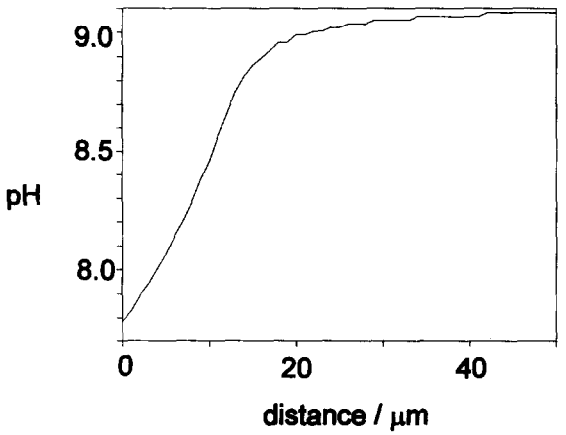

Fig. 5. pH–distance profile over a 40-μm silver iodide target in 1 mM KCN, 0.1 M KCl and 1 mM pH 9.0 phosphate buffer. The tip diameter was 15 μm and the x-axis is the absolute tip-to-surface distance.

higher buffer capacity. This indicates a lower iodide activity at the measuring membrane surface. As was mentioned earlier the anomalous behaviour could be explained by assuming that there is a difference between the bulk pH and the local pH at the electrode membrane surface. The extent of this pH difference could be estimated from the difference between the theoretical and experimental curves.

Scanning electrochemical microscopy with the potentiometric tip

Using scanning electrochemical microscopy with the pH measuring antimony tip, the existence of the local pH gradient was checked. An estimation of the thickness and shape of this diffusion layer was also attempted. An SECM experiment was carried out in the following manner. First the silver iodide target was placed in the cell. The tip was roughly positioned over the target manually, using the x–y piezoelectric motors. A telescopic lens was very helpful for this. (To avoid a major concentration change caused by the corrosion reaction in the small volume cell, small targets (diameter 40–80 μm) were used in these studies). Air-saturated cyanide-free buffer solution (4 ml) was introduced into the cell and using a -0.8 V measuring potential, the tip-target distance was adjusted and determined. As was indicated before, this was accomplished by following the oxygen reduction amperometric current intensity vs. Z direction step, distance curve and fitting it to the theoretical working curve data. To regain its pH measuring function the tip was polarised at 0.0 V for a few seconds. After this the potentiometric measuring mode was installed. Different buffered and unbuffered cyanide solutions were introduced and the microscopic experiments were performed.

Figure 5 shows the pH–distance profile over the centre of a 40-μm diameter silver iodide target. The solution contained 1 mM KCN, 0.1 M KCl and 1 mM pH 9.0 phosphate buffer. The decrease of pH near the silver iodide surface is apparent. Furthermore, the measured surface pH of ca. 7.8 is in reasonable agreement with the value estimated from Fig. 4 by considering the displacement on the pH axis of the E–pH curve in 10^{-3} M buffer from the curve in the most concentrated buffer. The inflection on the pH–distance curve is most likely due to the shielding effect of the tip (15 μm diameter) on the target at small distances. In other words, when the tip approaches too closely it blocks the cyanide transport to the surface so the corrosion process slows down. This steric hindrance affects the cyanide diffusion more than the pH equilibration.

As a control, the pH–distance curves were also recorded in cyanide-free solutions containing 100

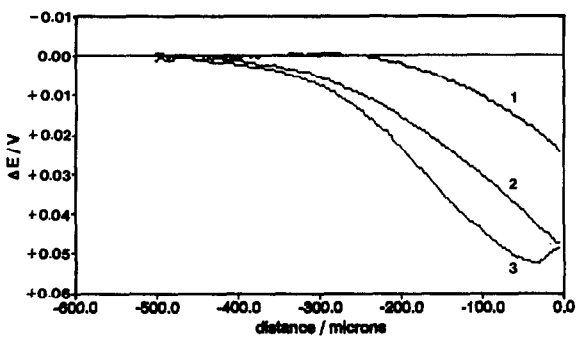

Fig. 6. ΔE–distance profiles over a silver iodide target in 1 mM phosphate buffer (pH 9.0) at different cyanide concentration levels. The antimony tip was 15 μm. The solution contained 0.1 M KCl also. Cyanide concentration: (1) 1 mM; (2) 3 mM; (3) 5 mM.

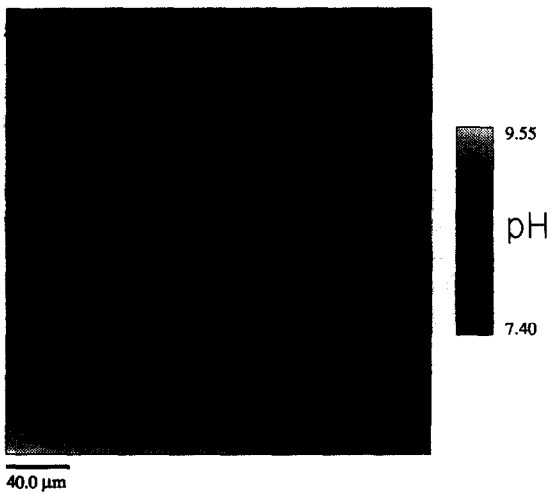

Fig. 7. Image of the pH profile over a 40 μm diameter silver iodide target. The gray scale shows the antimony tip potential corresponding to pH values; white corresponds to higher pH. The tip diameter was 15 μm. The solution contained 0.1 M KCl, 1 mM KCN and 10^{-4} M pH 9.0 phosphate buffer.

mM potassium chloride. No measurable difference could be observed in this experiment between the pH of the bulk solution and at the silver iodide target surface.

Figure 6 exhibits E vs. distance curves recorded over silver iodide surface with SECM incorporating a 2-μm antimony tip in 10^{-3} M phosphate buffer (pH 9) at 1, 3 and 5 mM KCN concentration levels. (The solutions also contained 0.1 M KCl in all cases.) Higher cyanide concentration results in higher corrosion rate which is clearly reflected on the ΔE vs. distance curves. ΔE in relevance to the ΔpH means the difference of the local and bulk electrode potential values of the antimony tip.

The above SECM experiment clearly proves that the corrosion reaction involves an appreciable pH change in the solution adjacent to the silver iodide surface when the buffer capacity is small. This validates the basic assumption made in the earlier explanation for the anomalous pH dependence of the cyanide electrode function observed in unbuffered media.

The SECM can provide a two-dimensional image of the silver iodide disk taking advantage of the pH change caused by the corrosion reaction. Figure 7 shows an image of a 40 μm diameter silver iodide target in 1 mM KCN, 0.1 M KCl and 0.1 mM phosphate buffer (pH 9.0). At the distance measured, the pH is about two units lower than in the bulk solution. The lower near surface pH in this image compared to Fig. 5 is consistent with the lower buffer capacity. The pH–electrode potential curves predict the existence in the case of higher cyanide concentration and unbuffered media of large pH differences (1–3) between the electrode surface and the bulk of the solution.

The support of this work by a grant from the US National Science Foundation (CHE 9214480) and by the Hungarian OTKA 5-346 is gratefully acknowledged.

REFERENCES

1 K. Tóth and E. Pungor, Anal. Chim. Acta, 51 (1970) 221.
2 E. Pungor and K. Tóth, Analyst, 95 (1970) 625.
3 P.L. Bailey, Ion-Selective Electrode Reviews, 1 (1970) 81.
4 I. Sekerka and J.F. Lechner, Water Res., 10 (1976) 479.
5 W.E. Morf, G. Kahr and W. Simon, Anal. Chem., 45 (1974) 1538.
6 D.H. Evans, Anal. Chem., 44 (1972) 875.
7 J. Koryta, Anal. Chim. Acta, 61 (1972) 329.
8 G.P. Bound, B. Fleet, H. von Storp and D.H. Evans, Anal. Chem., 45 (1973) 788.
9 A. Hulanicki and A. Lewenstam, Talanta, 24 (1977) 171.
10 M. Mascini, Anal. Chem., 45 (1973) 614.
11 M. Gratzl, F. Rakiás, G. Horvai, K. Tóth and E. Pungor, Anal. Chim. Acta, 102 (1978) 85.
12 G.A. Rechnitz and L. Lenado, Anal. Chem., 44 (1972) 468.
13 M. Gratzl, PhD Thesis, Budapest, 1984.
14 E. Pungor, M. Gratzl, L. Pólos, K. Tóth, M.F. Ebel, H. Ebel, G. Zuba and J. Wernisch, Anal. Chim. Acta, 156 (1984) 9.
15 A.J. Bard, F.R. Fan, D.T. Pierce, P.R. Unwin, D.O. Wipf, F. Zhou, Science, 254 (1991) 68.
16 J. Kwak and A.J. Bard, Anal. Chem., 61 (1989) 1221.
17 B.R. Horrocks, M.V. Mirkin, D.T. Pierce, A.J. Bard, G. Nagy and K. Tóth, Anal. Chem., 65 (1993) 1213.
18 S. Glab, A. Hulanicki, G. Edwall and F. Ingman, Crit. Rev. Anal. Chem., 21 (1989) 29.
19 H.A. Bicher and S. Onki, Biochim. Biophys. Acta, 255 (1972) 900.
20 Y. Matsumura, K. Kajino and M. Fujimoto, Membr. Biochem., 3 (1980) 99.
21 R.M. Wightman and D.O. Wipf, in A.J. Bard (Ed.), Electroanalytical Chemistry, Marcel Dekker, New York, 1988, Vol. 15.